

STATUS OF HIGH-EFFICIENCY KLYSTRON DEVELOPMENT FOR THE PLS-II AND PAL-XFEL*

S.J. Park[†], Y.J. Park, S.D. Jang, W.H. Hwang, K.R. Kim, Y.D. Joo, H.S. Han, C.D. Park,
Pohang Accelerator Laboratory, Pohang, Korea
J.H. Hwang, S.S. Jang, Physics Department, POSTECH, Pohang, Korea
H.S. Seo, D.H. Yu, S.Y. Hyun, Vitzrotech Co., Ltd., Ansan, Korea

Abstract

We are developing a high-efficiency klystron for use in the PLS-II (Pohang Light Source II) and the PAL-XFEL in the Pohang Accelerator Laboratory. Since the PLS-II and the PAL-XFEL are already running with ~ 70 klystron modulator systems, newly developed klystrons should be designed to fit into existing installation spaces and power supplies, and their overall lengths (< 2 m) and beam perveances (2 upervs) should not be changed. In order to achieve the high efficiency with aforementioned boundary conditions, we are going to adopt a multi-cell output cavity in which, unlike those of the the SLAC X-band and KEK C-band klystrons, the cell frequencies are independently tuned to provide maximum beam-to-rf power conversion. In this article we report on our physics and engineering design efforts to achieve the high efficiency with minimum instabilities.

INTRODUCTION

Two light sources are operating in the Pohang Accelerator Laboratory, They are the PLS-II (Pohang Light Source – II, a storage ring based 3rd generation light source) and the PAL-XFEL (a linac based 4th generation light source) which requires high-energy electron beams with energies 3 GeV and 10 GeV respectively. Here the microwave powers for accelerating electrons are provided by about 70 klystrons (output power 80 MW at 4 μ s, 60 Hz).

In order to establish stable supports for the klystron operation and maintenance, we have been performed government funded R&Ds which is expected to develop commercial-grade klystrons with improved performances.

R&D STRATEGIES

The klystrons are being developed to be fully compatible with existing facilities including modulators, waveguide networks, and mechanical/cooling systems. This means that the gun perveance should not deviate much from the current value (2 μ pervs), overall length should be about 2 meters. In spite of these constraints we are going to improve their performances including the efficiency and beam losses.

The R&D work is being performed in two phases. The first phase is to develop the “baseline” model (BM) with conventional design and minor performance improvements. But it should be deployed to the klystron gallery as soon as possible (2019 ~ 2020). The second phase is to

develop the “alternative” model (AM) with major performance improvements. By adopting a multi-cell output cavity the efficiency will be increased to $>55\%$. Also the beam losses (as well as radiation emission associated to them) will be greatly decreased with careful design of gun & focusing optics and beam-cavity interaction dynamics. Table 1 compares the two models.

Table 1: Comparison of Baseline and Alternative Models

	Baseline Model	Alternative Model
Target Efficiency	45%	$>55\%$
Output Cavity Type	Single Cell	Multi Cell
Surface Electric Field	Similar to Toshiba E3712	Half of Baseline
Beam Voltage/Current for 80-MW Output	400 kV / 478 A	358 kV / 407 A
Cathode Lifetime	Max. 80,000 hr	40% longer than baseline
Risk	-	Instabilities
Beam Losses	a few %	0%

Fig. 1 shows energy and beam profiles for the AM with a 3-cell output cavity, calculated by the FCI (Field-Charge Interaction [1]) code. Owing to the extended interaction at the output cavity gaps, much more portion of kinetic energy of the electron beam is converted to the RF energy. This is achieved at moderate transverse beam blow-up.

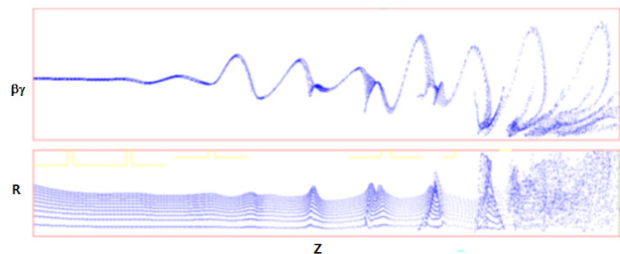


Figure 1: Energy and Beam Profiles of the AM with 3-cell output cavity (calculated by the FCI code).

Figure 2 shows the dependence of klystron operation parameters on cell tunings, and the transfer characteristic (also calculated by the FCI code).

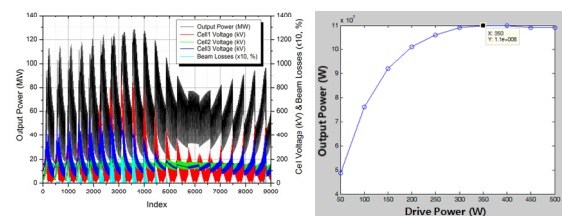


Figure 2: Dependence of AM operation parameters on cell tunings (left) and transfer characteristic (right).

In Fig. 3 the design of the 3-cell output cavity is seen. Cell-to-cell coupling is done with the H-coupling. Two waveguide couplers are symmetrically attached to the last cell.

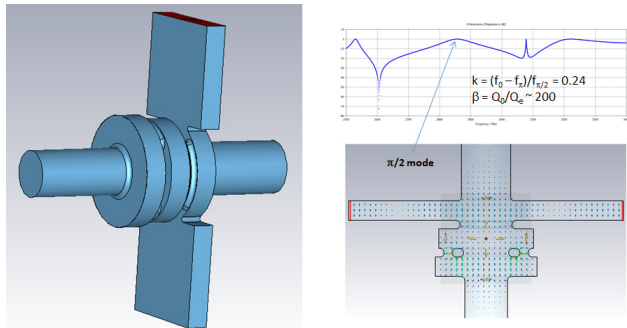


Figure 3: 3-Cell Output Cavity for the AM (Alternative Model).

R&D PROGRESSES

In this article we would like to focus on design work. Fabrication technologies so far accumulated in this laboratory were reported in a previous publication [2]. They are now being transferred to the industry.

Gun Optics

Cathode development is out of the scope of this work and we will use a commercial one. We are going to procure the Scandate cathode with existing dimensions. Gun optics is designed with the use of the EGUN code [3]. The CST particle studio (CST-PS) [4] is also used to cross-check the result from the EGUN code. Cold dimension is obtained by the ANSYS code. The difference between the hot and cold dimensions is as large as 2.4 mm at the downstream end of the Whenelet electrode. This well corresponds to the measured value [5]. Table 2 summarizes the hot and cold dimensions as obtained by the ANSYS calculation.

Table 2: Comparison of Hot and Cold Dimensions for the Klystron Gun

	Cold Dimension	Hot Dimension
Cathode Spherical Radius (mm)	73.69	74.02
Cathode Radius (mm)	44.37	44.57
Axial Expansion of Whenelet (mm)		2.4
Radial Expansion of Whenelet (mm)		0.75

Figure 4 is the electron trajectories calculated by the EGUN as well as the CST-PS. Optics parameters obtained from the two codes are compared in Table 3.

Table 3: Comparison of Optics Parameters Calculated by the EGUN and the CST-PS

	EGUN	CST-PS
Microperveance	2.05	1.91
Waist Position from Cathode (mm)	160	172
Scalloping	0.20	0.25

In Table 3, the parameter “scalloping” is defined by,

$$Scalloping = \frac{r_{max} - r_{min}}{(r_{max} + r_{min})/2} \quad (1)$$

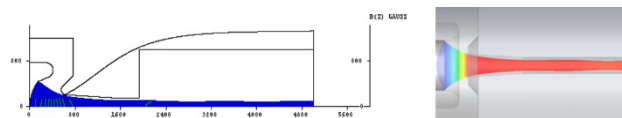


Figure 4: Electron trajectories calculated by the EGUN (left, axes scales are in /0.1mm) and the CST-PS (right) codes.

Multipacting in the Gun Ceramic Insulator

Electron multipacting at the inner surface of the gun ceramic insulator (usually Al₂O₃) is one of the major causes of the gun arcing. Important source of the electrons is the so-called “triple point” (TP) which is inevitably formed at the bottom of the ceramic insulator. We simulated the electron multipacting originating from the TP using the CST-PS (See Fig. 5).

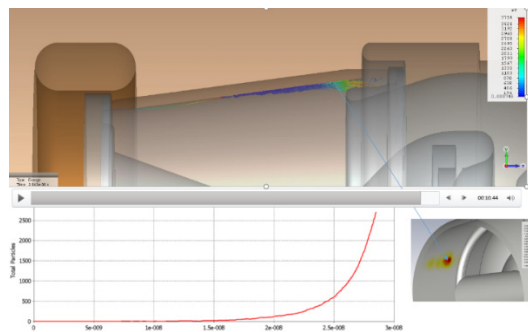


Figure 5: Multipaction of an electron emitted from the triple point (TP) at the bottom of the ceramic insulator (ceramic-welding lip-vacuum junction). A spot of intense charge deposition is indicated at the lower right insertion.

Electron multipaction strongly depend on the secondary electron emission (SEE) yield as well as the electric field distribution near the TP. The SEE yield depend on the surface condition and can be greatly reduced by coating with some material with low SEE yield, such as the TiN. This is one of the practical ways to suppress the multipaction but more fundamental solution to the problem would be electrically shielding the TP to reduce the electric field around it. This would not only suppress electron emission from the TP but also prevent emitted electrons to propagate downstream. A practical implementation of the shielding is suggested in Fig. 6 together with electron trajectories around the TP. The electron trapping shown in

Fig. 6 is due to the reduced longitudinal electric field (E_z) near the TP. The magnitudes of longitudinal and transverse electric fields near the TP for the unshielded and shielded cases are compared in Fig. 7.

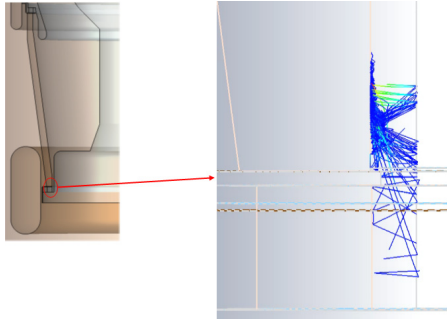


Figure 6: Possible shielding of the TP by cathode stem (left). Due to the reduced longitudinal electric field electrons emitted from the TP are trapped near it (right).

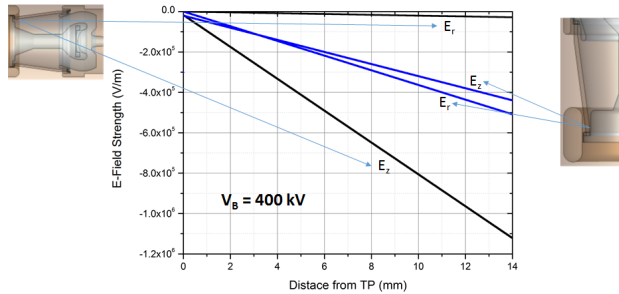


Figure 7: Comparison of electric field distributions near the TP for unshielded (black lines) and shielded (blue lines) cases.

General PIC Simulation of Beam-Cavity Interaction

The beam-cavity interaction was simulated using the CST-PS. This produced useful information to understand the physical processes and to improve the klystron performances. For example, it was found that beam losses at the output gap were associated with transverse beam blow-up caused by abrupt deceleration of particles. Beam losses at the output gap would be greatly reduced in the AM in which the multi-cell output cavity used. This is because the decelerations take place gradually limiting the beam blow-up to a certain level.

Figure 8 is the time evolution of the longitudinal phase space for all the particles. The specific example is with large enough drive power (300 W) making the beam bunching fully saturated and the decelerating field at the output cavity gap large enough to cause some (< 1%) particles reflected to upstream direction. Some of the reflected particles are reflected again to downstream and trapped between the penultimate and the output cavities. Possible klystron instabilities associated with these trapped particles should be investigated.

Figure 9 is the heat distributions for various drive powers in the collector. It was found that when there is no drive

power the heat is concentrated to a specific region, which should be avoided to prevent possible local melting.

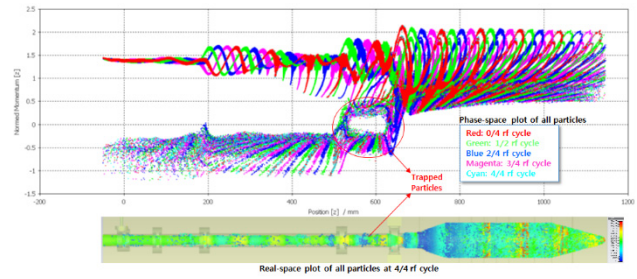


Figure 8: Time evolution (in a quarter RF cycle intervals) of longitudinal phase space for all particles (~3.4 million). A snapshot of real-space is also shown. Trapped particles between the penultimate and output cavities are clearly shown.

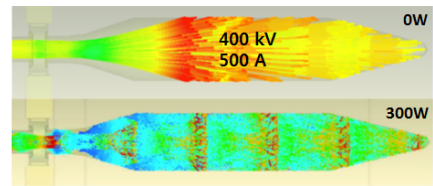
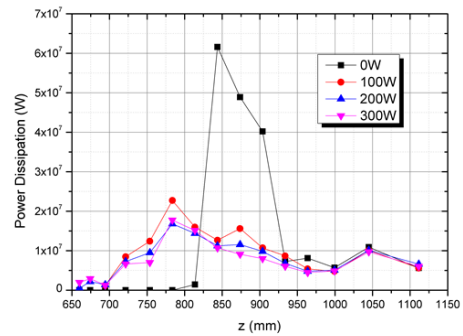


Figure 9: Power dissipation vs. z in the beam collector for various drive powers. Real-space plots for all particles are also shown.

CONCLUSION

We have been performing R&Ds to develop high-power klystrons to support stable operation and maintenance of the PLS-II and the PAL-XFEL. The work has well progressed to achieve high-efficient klystron design with considerable engineering details. Technology transfer to industry is also being done.

ACKNOWLEDGEMENT

The work was supported by the National R&D Program (grant number: 2016R1A6B2A01016828) through the National Research Foundation of Korea (NRF) funded by the Ministry of Science, ICT and Future Planning, Korea.

REFERENCES

[1] T. Shintake, NIM-A 363, pp. 83-89 (1995).
 [2] S.J. Park *et al.*, JKPS 48(4), pp.786-790 (2006).
 [3] W.B. Herrmannsfeldt, SLAC-331 (1988).

[4] <http://www.cst.com>

[5] S. J. Park *et al.*, LINAC2002, pp. 196-198 (2002).